Science Translational Medicine AAAS

Dendrimer-Based Postnatal Therapy for Neuroinflammation and Cerebral Palsy in a Rabbit Model
Sujatha Kannan *et al.*
Sci Transl Med **4**, 130ra46 (2012);
DOI: 10.1126/scitranslmed.3003162

Editor's Summary

One Hop at a Time

Cerebral palsy (CP) is a developmental disorder caused by injury to a baby's brain while it is still developing, either in the womb or during the early months of life, but is often not diagnosed until children are 2 to 3 years of age. There is no cure for CP, and the best option for affected children is intensive physical therapy to improve motor skills. Now, Kannan *et al.* have designed a dendrimer-based therapeutic for treating this developmental disorder in baby rabbits (kits), opening the door to new treatment options in humans.

The authors chose to use the rabbit model of CP, which replicates the neuroinflammation seen in human brains as well as the motor deficits in children. To generate this model, Kannan and colleagues injected *Escherichia coli* toxin into the rabbit mother's uterus at about 90% term gestation. When the kits were born, they were administered either a saline solution, a free drug known as NAC (*N*-acetyl-l-cysteine), or a dendrimer-NAC (D-NAC) conjugate. This postnatal "rescue" with D-NAC, given on day 1 of life, allowed CP kits to develop normally, able to walk and hop. The successfully treated kits also had neuron counts and low inflammation similar to healthy control animals. By comparison, NAC alone or saline had no effect. The authors believe that conjugating NAC to the dendrimers promoted greater uptake by activated microglia and astrocytes, with no toxicity to surrounding neurons. Although still in preclinical testing in rabbits, this dendrimer-drug conjugate shows promise for postnatal treatment of babies suspected of having CP.

Science Translational Medicine (print ISSN 1946-6234; online ISSN 1946-6242) is published weekly, except the last week in December, by the American Association for the Advancement of Science, 1200 New York Avenue NW, Washington, DC 20005.

CEREBRAL PALSY

Dendrimer-Based Postnatal Therapy for Neuroinflammation and Cerebral Palsy in a Rabbit Model

Sujatha Kannan,[1,2]*† Hui Dai,[1,2] Raghavendra S. Navath,[1,3] Bindu Balakrishnan,[1,2]* Amar Jyoti,[1,2]* James Janisse,[4] Roberto Romero,[1†] Rangaramanujam M. Kannan[1,3†‡]

Cerebral palsy (CP) is a chronic childhood disorder with no effective cure. Neuroinflammation, caused by activated microglia and astrocytes, plays a key role in the pathogenesis of CP and disorders such as Alzheimer's disease and multiple sclerosis. Targeting neuroinflammation can be a potent therapeutic strategy. However, delivering drugs across the blood-brain barrier to the target cells for treating diffuse brain injury is a major challenge. We show that systemically administered polyamidoamine dendrimers localize in activated microglia and astrocytes in the brain of newborn rabbits with CP, but not healthy controls. We further demonstrate that dendrimer-based *N*-acetyl-L-cysteine (NAC) therapy for brain injury suppresses neuroinflammation and leads to a marked improvement in motor function in the CP kits. The well-known and safe clinical profile for NAC, when combined with dendrimer-based targeting, provides opportunities for clinical translation in the treatment of neuroinflammatory disorders in humans. The effectiveness of the dendrimer-NAC treatment, administered in the postnatal period for a prenatal insult, suggests a window of opportunity for treatment of CP in humans after birth.

INTRODUCTION

Cerebral palsy (CP) is a broad term encompassing a group of disorders involving variable degrees of motor, sensory, and cognitive impairment that occur as a result of an injury/insult to the developing fetal or infant brain (*1*). This chronic childhood disability may result from diverse etiologies, with a prevalence of 3.3 per 1000 children (*2*), and is associated with substantial social, personal, and financial burdens (*3*). Intrauterine infection and inflammation are risk factors for the development of periventricular leukomalacia (PVL) and CP in the neonate (*4*–*7*). PVL, the pathophysiological mechanism proposed for the development of CP in humans, is characterized by focal necrosis around the ventricles and diffuse microglial and astrocyte activation in the immature white matter (*8*). Microglia, immune cells in the brain, play an important role in remodeling and growth in the fetal and postnatal period (*9*). Activation of these cells can result in an exaggerated inflammatory response with formation of free radicals, excitotoxic metabolites, and proinflammatory cytokines, leading to brain injury (*10*, *11*). In severe inflammation, astrocytes that normally participate in the protection of neurons and in preventing oxidative injury are unable to maintain their neuroprotective role (*12*).

Treatment of disorders such as CP is challenging for several reasons. Inflammation and injury are often diffuse in the white matter, precluding local brain delivery. Furthermore, clinical diagnosis of CP is made well after birth, so postnatal treatment of a prenatal injury to the brain is not expected to result in improvement in motor function. Finally, transport of drugs across the blood-brain barrier (BBB) is difficult to achieve. We hypothesized that a postnatal therapeutic strategy targeting activated microglia and astrocytes for sustained attenuation of ongoing neuroinflammation would improve outcomes in an animal model of CP.

Taking advantage of the differences between cellular localization of nanomaterials in healthy and diseased tissues may help address these treatment challenges. Here, we used polyamidoamine (PAMAM) dendrimers as vehicles for delivery of *N*-acetyl-L-cysteine (NAC). NAC, an antioxidant and anti-inflammatory agent, has a long history of clinical use as an antidote for acetaminophen poisoning (doses from 50 to 150 mg/kg) (*13*) and is being explored in several ongoing clinical trials for potential neuroprotective effects in autism spectrum disorders (ClinicalTrials.gov IDs: NCT00453180 and NCT00627705), in pregnant women for the treatment of maternal and fetal inflammation (NCT00397735 and NCT00724594), in Alzheimer's disease (NCT01320527), and in animal models of perinatal brain injury (*14*, *15*). Dendrimers are viewed as synthetic biomimics of globular proteins, with versatile tailorable surface functionalities. They are being explored in preclinical studies for cancer therapy, inflammation, and targeted delivery applications (*16*–*19*). We have previously shown that hydroxyl-terminated PAMAM dendrimers localize in activated microglia and astrocytes when injected into the subarachnoid space of neonatal rabbit brains with a CP phenotype, but not in age-matched healthy controls (*20*). Building upon this work, we investigated whether these dendrimers can localize in activated microglia and astrocytes even when administered systemically to newborn rabbits with neuroinflammation and motor deficits. In addition, we asked whether delivering NAC to activated microglia and astrocytes using these dendrimers would lead to improvements in motor function. To this end, we show that NAC conjugated to the PAMAM dendrimer, administered intravenously on day 1 of life to rabbit kits with CP, resulted in significant

[1]Perinatology Research Branch, *Eunice Kennedy Shriver* National Institute of Child Health and Human Development, National Institutes of Health, Detroit, MI 48201, USA. [2]Department of Pediatrics, Children's Hospital of Michigan, Detroit Medical Center, Wayne State University, Detroit, MI 48201, USA. [3]Department of Chemical Engineering and Material Science, Wayne State University, Detroit, MI 48201, USA. [4]Department of Family Medicine and Public Health Sciences, Wayne State University, Detroit, MI 48201, USA.
*Present address: Department of Anesthesiology and Critical Care Medicine, Johns Hopkins University School of Medicine, Baltimore, MD 21287, USA.
†To whom correspondence should be addressed. E-mail: krangar1@jhmi.edu (R.M.K.); skannan3@jhmi.edu (S.K.); romeror@mail.nih.gov (R.R.)
‡Present address: Center for Nanomedicine/Wilmer Eye Institute, Ophthalmology, Johns Hopkins University School of Medicine, Baltimore, MD 21287, USA.

improvement in motor function along with a decrease in markers of neuroinflammation and oxidative injury by day 5 of life. This study suggests that targeted therapy of drugs using dendrimers may be effective in the treatment of neuroinflammatory disorders.

RESULTS

Preparation, characterization, and biodistribution of dendrimer-NAC conjugates

NAC was conjugated to generation-4, hydroxyl-terminated PAMAM dendrimers ("D"), [D-$(OH)_{64}$], using a disulfide linker, through a four-step reaction (Fig. 1 and fig. S1) (Supplementary Methods). In the first two steps, a bifunctional dendrimer [$(HO)_{39}$-D-$(GABA\text{-}NH_2)_{25}$, **4**] with 25 reactive amines was synthesized using our previously published protocol (*21*). The intermediate **4** was reacted with the heterobifunctional cross-linker *N*-succinimidyl-3-(2-pyridyldithio)-propionate (SPDP) to yield amide-linked 2-pyridyldithiopropanoyl (PDP)–functionalized dendrimer, [$(HO)_{39}$-D-$(GABA\text{-}PDP)_{25}$, **5**]. The appearance of aromatic thiopyridine protons in ^{1}H NMR (nuclear magnetic resonance) confirmed the formation of PDP-functionalized dendrimer **5**. In the final step, **5** was treated with water-soluble NAC in phosphate-buffered saline (PBS) solution (pH 7.4) to obtain the desired conjugate with a disulfide linkage between the drug and the dendrimer (D-NAC, **1**). The characteristic peaks in ^{1}H NMR spectrum of **1** corresponding to the dendrimer, NAC, and the linker confirm the formation of the product and the presence of disulfide bond between the dendrimer and NAC (fig. S1A) (*22*, *23*). The drug payload on the dendrimer was estimated by NMR and MALDI-TOF (matrix-assisted laser desorption/ionization–time-of-flight) mass spectrometry to be 19% (suggestive of 20 molecules of NAC) (table S1 and fig. S1B). The reverse-phase high-performance liquid chromatography (HPLC) chromatogram of D-NAC **1** at 210 nm shows a relatively narrow peak, different from that of the starting materials and intermediates, suggesting a relatively pure conjugate nanodevice (fig. S1C). The ζ potential changed from −2.1 mV for the starting dendrimer to −10.6 mV for the D-NAC **1** conjugate, due to surface modification with NAC, resulting in some carboxylic acid end functionalities. Particle size analysis by dynamic light scattering (DLS) showed that D-NAC is larger in size (5.4 nm) than D-OH **2** as expected, owing to higher molecular weight of the conjugate.

The hydroxyl-terminated PAMAM dendrimers used in this study are nontoxic, nonimmunogenic, and are cleared intact through the kidneys (*16*, *24*). Biosafety of the dendrimer after systemic administration (550 mg/kg) on day 1 was evaluated in healthy newborn kits at days 5 and 15 of age. There was no change in renal and hepatic functions or neurobehavior noted at both time points when compared to healthy kits administered PBS (table S2 and fig. S2). Liver enzymes remained normal, indicating that there was no hepatocellular injury with dendrimer administration. Ten percent of this amount was used as the maximum dendrimer dose in the present study.

In vitro NAC release from the D-NAC conjugate

Glutathione (GSH)–cleavable disulfide linkers were used between the drug and the dendrimer to enable intracellular release (*22*, *23*). At physiological conditions, in the absence of GSH, the conjugate was stable without releasing NAC over a 72-hour period. In vitro release of NAC was investigated at seven different GSH concentrations starting from 2 μM (plasma level) to 10 mM (intracellular levels) (Supplementary Methods). At extracellular and plasma GSH levels (2 μM), the conjugate did not release measurable NAC. As the GSH level was increased, proportionately more of NAC was released (fig. S3). At intracellular GSH concentrations (2 and 10 mM), the conjugate readily released the drug (>80% in 100 min), which could be detected mostly as free NAC, and as NAC-GSH to a smaller extent within 40 min. This indicated that the use of a disulfide linker enabled rapid release of NAC from the conjugate, but only when it was exposed to an intracellular GSH-rich environment (*22*, *23*). The mechanism of GSH-based release from dendrimer conjugates has been described previously (*23*). Reported GSH levels in microglia (~25 mM) and astrocytes (~4 to 20 mM) are well within the range shown for drug release from the conjugate (*25*). Even if the intracellular GSH levels were reduced significantly due to inflammation, there will still be sufficient GSH to release the drug.

In vivo brain biodistribution of dendrimers

All in vivo studies were performed with a previously described rabbit model, where CP is induced by maternal intrauterine endotoxin administration (*26*, *27*). Fluorescein-labeled dendrimer (D-FITC) was administered intravenously to newborn kits, and brains were examined after 24 hours. D-FITC was found to colocalize in activated

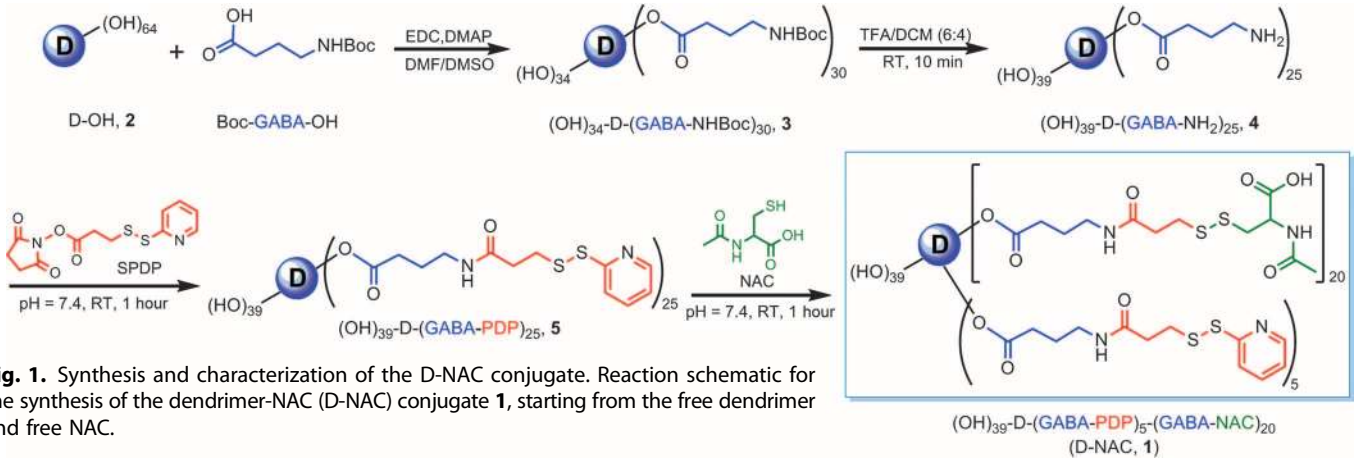

Fig. 1. Synthesis and characterization of the D-NAC conjugate. Reaction schematic for the synthesis of the dendrimer-NAC (D-NAC) conjugate **1**, starting from the free dendrimer and free NAC.

microglia and astrocytes in the periventricular region (PVR), in kits with CP, but not in healthy age-matched controls (Fig. 2). This increased brain uptake in CP kits was also consistent with results from positron emission tomography (PET) imaging of ^{64}Cu-labeled dendrimer. An increase in tracer activity was seen in CP kits injected with ^{64}Cu-dendrimer but not in controls (fig. S4). Very little uptake was seen in the control and CP kits injected with $^{64}CuCl_2$ alone. This selective localization in activated microglia and astrocytes was similar to that noted upon subarachnoid administration in CP kits and upon intravitreal administration in a rat model of neuroinflammation-induced retinal degeneration (*19*, *20*).

Impairment in BBB integrity was observed in CP kits on day 1 of life. This was demonstrated by decreased occludin expression, indicating loss of tight junction proteins and increased permeability evidenced by extravasation of Evans blue–albumin complex (Fig. 3).

D-NAC therapy improves motor function in CP kits

To determine whether targeting NAC to areas of neuroinflammation results in improved motor function, we randomly treated littermates with CP with NAC at 10 mg/kg (NAC_10), NAC at 100 mg/kg (NAC_100), D-NAC with NAC at 1 mg/kg (D-NAC_1), D-NAC with NAC at 10 mg/kg (D-NAC_10), dendrimer alone (delivery vehicle control), or PBS (negative control). A total of 69 kits from 14 dams that underwent laparotomy and intrauterine endotoxin administration were used for the study. To minimize the variation between treated animals, we administered kits from the same litter with different therapies. The healthy control group consisted of kits born to dams that had no endotoxin intervention (healthy control). All treatments were administered intravenously as a single dose within 6 hours after birth (day 1). Using modifications of observational motor function scores for rabbits, we evaluated the kits in a blinded manner for change in motor function on day 5 (during the peak myelination period in rabbits), as described in Materials and Methods (*28*, *29*).

Endotoxin-exposed kits were born with impaired motor function involving inability to take steps, decreased coordination, impaired balance, and hypertonia of the hindlimbs suggestive of a phenotype of CP as described previously in this model (*27*, *30*). The endotoxin-exposed kits had similar motor function scores on day 1 of life, whereas healthy control kits that had no intervention were normal and had significantly better motor function (Fig. 4A and movies S1 and S2). The most favorable response in motor function from day 1 to day 5 was seen in kits treated with D-NAC_10 (Fig. 4A), manifested by marked improvement in coordination and motor control while hopping and

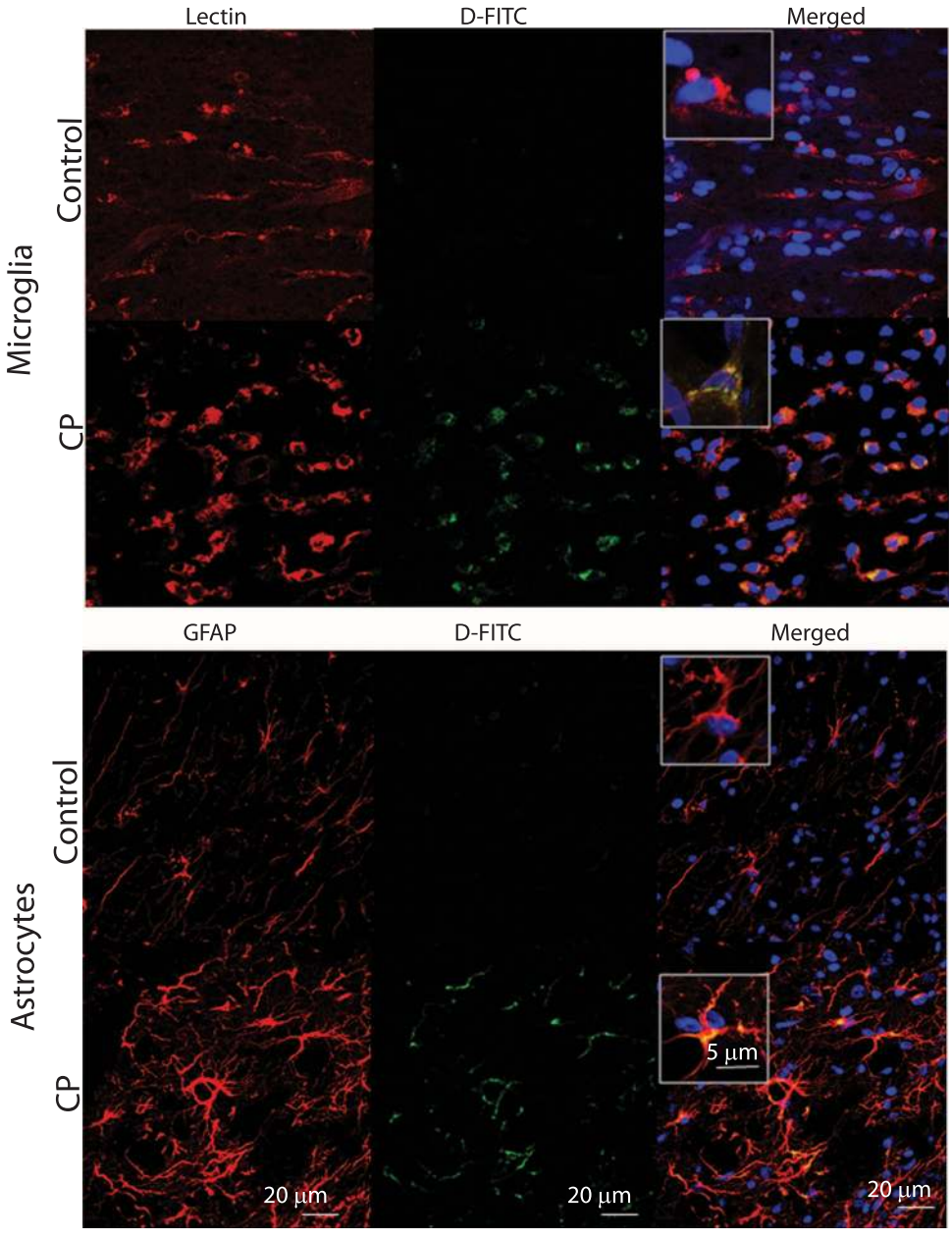

Fig. 2. Cellular localization of FITC-labeled dendrimer in the brains of 1-day-old newborn healthy (control) and CP rabbits upon intravenous administration. Representative images of the PVR from healthy control and endotoxin-exposed newborn rabbits (CP group). Microglia were identified by staining with tomato lectin (red in microglia panels). Astrocytes were stained with an anti–glial fibrillary acidic protein (GFAP) antibody (red in astrocyte panels). Images were merged to observe colocalization of dendrimer-FITC (D-FITC) with microglia and astrocyte cell types. Nuclei were stained with 4′,6-diamidino-2-phenylindole (DAPI) (blue). Scale bars, 20 μm. Inset shows microglia and astrocytes at higher magnification (scale bar, 5 μm).

taking steps (movie S3). No improvement in motor function was seen with PBS (negative control) (movie S2) or dendrimer (vehicle control) (movie S4). A small improvement in mean locomotion score was also seen in kits treated with NAC_10 (movie S5). However, the motor function on day 5 for the D-NAC_10 group was significantly better than that for the groups treated with equivalent dose of the drug alone (NAC_10) and a 10-fold higher dose of the free drug (NAC_100) (Fig. 4A). Locomotion scores for kits treated with D-NAC_10 approached that of healthy control kits born to mothers with no surgical intervention, but were statistically lower than the healthy controls on day 5. Mean locomotion score on day 5 was 7.5 [95% confidence interval (CI), 7.07 to 7.92] for controls and 6.44 (95% CI, 5.75 to 7.14) for the D-NAC_10 group ($P = 0.03$). Change in mean score from baseline to day 5 was greatest for kits treated with D-NAC_10 ($P \leq 0.01$ for D-NAC_10 versus PBS, dendrimer, NAC_10, and NAC_100), with no significant difference between D-NAC_10 and healthy controls (Fig. 4A).

Hindlimb tone was assessed using the modified Ashworth score as previously described (*28*). Values were compared between the treatment groups on days 1 and 5 in a subset of newborn rabbits exposed to endotoxin in utero ($n = 5$ kits per group). On day 1 of life, all endotoxin kits had hindlimb hypertonia and there was no significant difference in the degree of hypertonia between any of the treatment groups. A significant improvement in tone from day 1 to day 5 was seen only in kits treated with D-NAC (1 and 10 mg/kg) when compared to PBS ($P < 0.001$) (Fig. 4B). The maximum improvement in tone from baseline was noted in kits treated with D-NAC_10. There was no significant difference in the change in tone between PBS and NAC_10 or NAC_100 from day 1 to day 5.

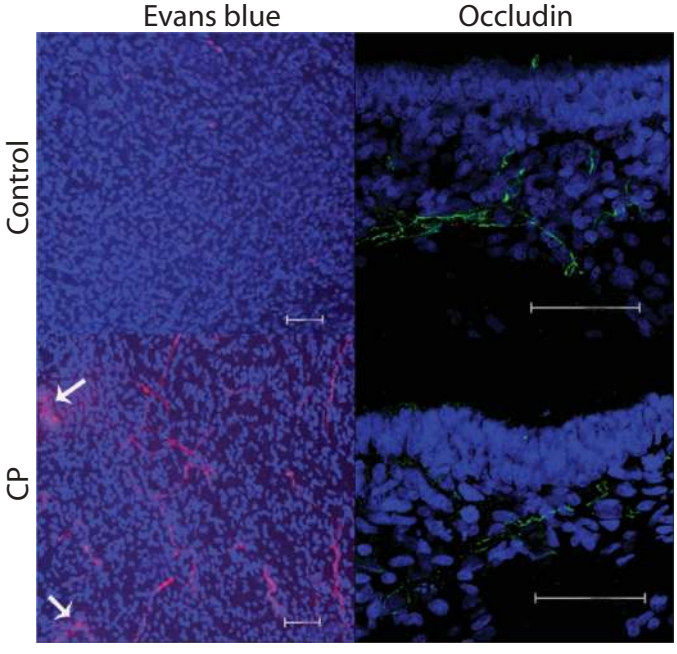

Fig. 3. Evaluation of BBB in newborn rabbits with CP. Representative brain sections in the PVR from healthy and CP kits on day 1 of life ($n = 3$ per group). The Evans blue–albumin complex is seen as red fluorescence. Arrows point to extravasation of Evans blue–albumin complex into the parenchyma in CP kits. Occludin staining is with Alexa Fluor 488 green. Nuclei were stained with DAPI (blue). Scale bars, 50 μm.

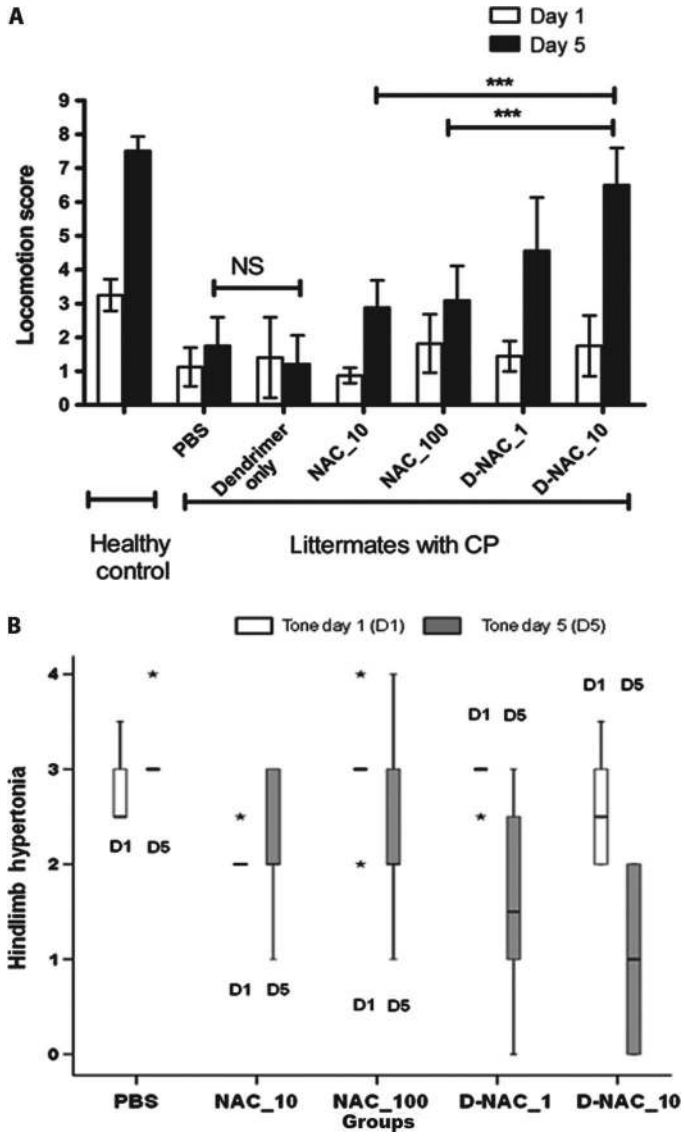

Fig. 4. Motor function and tone in healthy control and CP kits. (**A**) Locomotion score on day 5 after a single intravenous treatment within 6 hours of birth (day 1) of newborn rabbit kits. Data are means and 95% CI for each treatment group on days 1 and 5 ($n = 6$ to 16 endotoxin-exposed kits per treatment group, $n = 12$ healthy kits from four litters). See movie S1 (healthy control), movie S2 (PBS treatment), movie S3 (D-NAC_10), movie S4 (dendrimer alone), and movie S5 (NAC_10) for representative locomotor changes between day 1 and day 5. ***$P < 0.001$; NS, not significant, for locomotion score on day 5. (**B**) Evaluation of hindlimb tone in rabbit kits on days 1 and 5 of life. Hindlimb tone was assessed in a subset of endotoxin kits after treatment with PBS, NAC (10 and 100 mg/kg), or D-NAC (1 and 10 mg/kg) ($n = 5$ kits per group) as previously described for newborn rabbits: "0" indicates normal tone; "1" indicates slight increase in muscle tone when the limb is moved in extension or flexion; "2" indicates more marked increase in muscle tone through most of the range of movement but affected part is easily moved; "3" indicates considerable increase in tone, passive movement is difficult; and "4" indicates limb is rigid in flexion or extension (*28*). The values are represented as median (indicated by dark horizontal line), interquartile range (box), minimum and maximum values (whiskers), and extremes in values or outliers (*).

Kit weight gain and survival

Because the inflammatory stimulus occurs 3 days before birth, all endotoxin kits have intrauterine growth restriction with lower birth weights compared to healthy control kits on day 1 of life ($P < 0.001$). There was no significant difference in day 1 weights between the different endotoxin-exposed treatment groups (table S3). There was no significant difference in weight gain from day 1 to day 5 between healthy controls and NAC- or D-NAC–treated CP animals, but PBS- and dendrimer-treated animals gained less weight than the kits treated with NAC or D-NAC ($P < 0.01$) (table S3). An increased catabolic rate due to ongoing inflammation may account for the lower weight gain in kits treated with PBS and dendrimer alone. Survival up to day 5 was similar between all endotoxin (CP) groups and ranged from 77 to 85%.

D-NAC suppresses markers of oxidative injury and inflammation in the brains of CP kits

To understand how D-NAC improved locomotion in the CP rabbit brain, we examined the effect of the dendrimer-drug conjugate on oxidative injury, inflammation, microglial activation, myelination, and neuronal cell loss. Oxidative injury was assessed by quantifying markers of free radical injury to lipid, intracellular proteins, and RNA in the PVR of brains removed from 5-day-old rabbits treated on day 1 (Fig. 5A). The PVR was evaluated owing to the increased presence of activated microglia seen in this region in endotoxin kits with CP (*26*, *27*) and because of the frequent involvement of this region in patients with CP (*8*). Activated microglia release proinflammatory cytokines and free radicals, which can damage both neurons and myelin (*10*, *11*). GSH is a major intracellular antioxidant in the brain that helps protect cells by reducing free radicals. The concentration of GSH is primarily dependent on the availability of cysteine (*31*). NAC, a precursor for cysteine, helps replenish GSH in cells. Here, total GSH levels provided an indirect measure of the amount of NAC present in the brain after treatment with D-NAC and free NAC. An increase in GSH levels comparable to that of healthy control kits was seen in CP kits treated with D-NAC_1, D-NAC_10, and with the highest dose of free drug (NAC_100), whereas treatment with NAC_10 and dendrimer alone had no effect (Fig. 5A). This indicates that NAC is released from the dendrimer conjugate in the brain.

4-Hydroxynonenal (4-HNE), a highly reactive aldehyde formed after oxidative injury to lipids (*32*), was significantly lower in the brain of kits treated with D-NAC_10 when compared to those that received the equivalent dose of drug alone (NAC_10) (Fig. 5A).

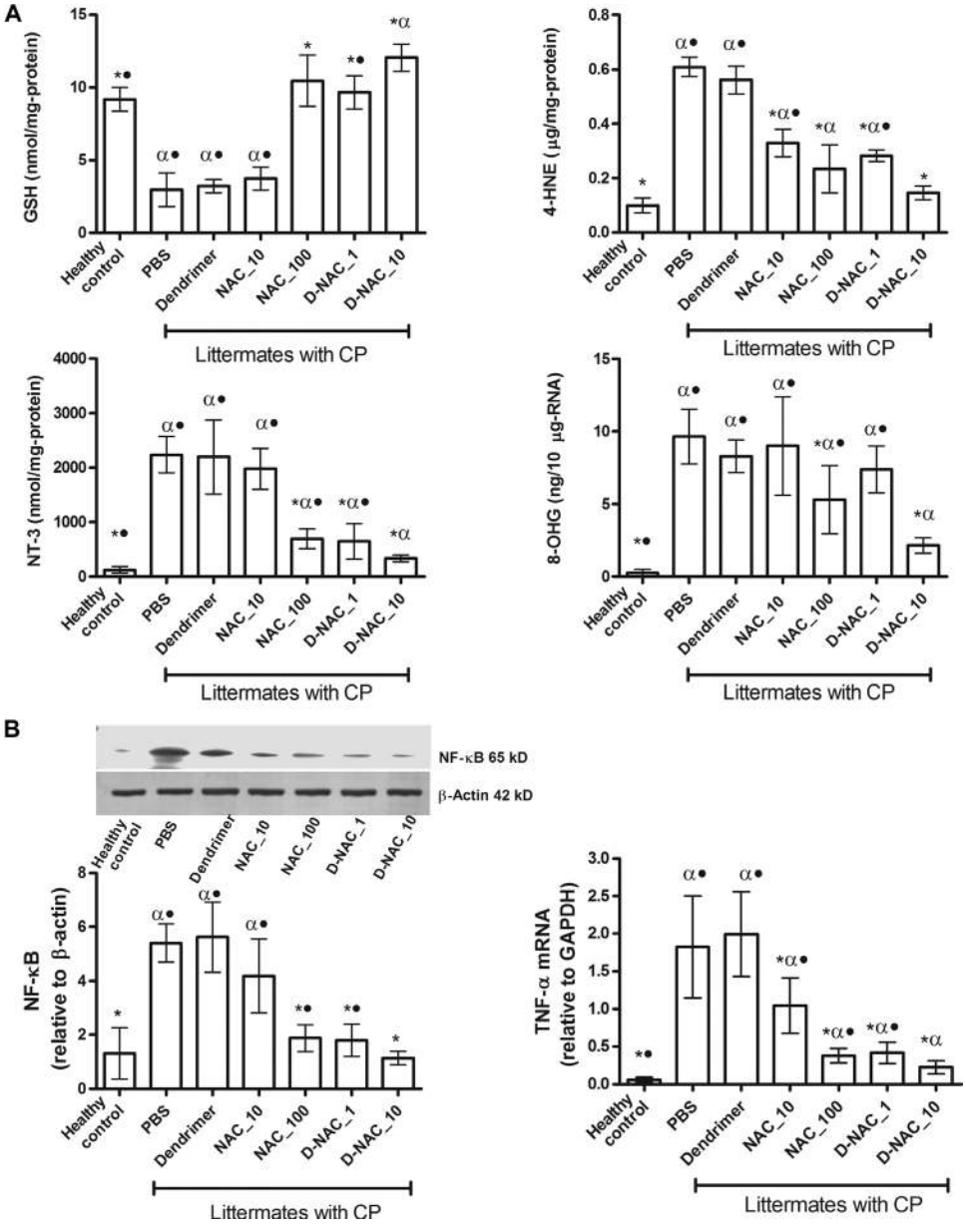

Fig. 5. Oxidative injury and inflammation on day 5 after treatment on day 1. (**A**) Markers of oxidative injury in PVR of the brain. Glutathione (GSH), 4-hydroxynonenal (4-HNE), 3-nitrotyrosine (NT-3), and 8-hydroxyguanosine (8-OHG) concentrations were measured in healthy and CP rabbits after treatment (n = 6 to 7 kits for healthy controls and 4 to 11 kits for the treatment groups, for each measure). Graphs denote the mean value with 95% CI for each group. *$P < 0.01$ when compared to PBS; $^{\alpha}P < 0.01$ when compared to healthy control; $^{\bullet}P \leq 0.01$ when compared to D-NAC_10. (**B**) NF-κB and TNF-α mRNA levels in the PVR of the brain. Western blot of NF-κB p65 expression was quantified and normalized to β-actin. TNF-α mRNA was quantified and normalized to GAPDH expression. Graphs denote the mean value with 95% CI for each group. *$P < 0.01$ when compared to PBS; $^{\alpha}P < 0.01$ when compared to control; $^{\bullet}P \leq 0.05$ when compared to D-NAC_10.

Oxidative injury to proteins by $ONOO^-$ (peroxynitrate), one of the most potent free radicals, was measured by evaluating 3-nitrotyrosine (NT-3), which is produced by nitration of tyrosine residues on proteins (*33*). NT-3 levels decreased upon treatment with D-NAC_10 when compared to PBS- and free NAC–treated kits (Fig. 5A), indicating an improvement in oxidative injury with D-NAC_10 therapy. Finally, levels of 8-hydroxyguanosine (8-OHG), an early and sensitive marker for RNA oxidation in various neurodegenerative disorders (*34*), were significantly reduced with D-NAC_10 in CP littermates when compared to free NAC alone even at the highest dose (Fig. 5A). The greatest decrease in oxidative injury was seen in kits treated with D-NAC_10, which was two- to sixfold better than the equivalent dose of drug alone. D-NAC_10 was significantly better than 10 times the dose of the drug alone in suppressing NT-3 and 8-OHG.

NAC is known to suppress activation of nuclear factor κB (NF-κB), which induces transcription of proinflammatory genes, such as tumor necrosis factor–α (TNF-α) (*35*). TNF-α is responsible for microglial proliferation and activation perpetuating the inflammatory process in the brain (*8*, *11*). A single dose of D-NAC_10 led to a 3.5-fold decrease in NF-κB expression when compared to equivalent dose of the free drug (NAC_10) (Fig. 5B). A significant decrease in mRNA expression of TNF-α was also noted in the brain of kits treated with D-NAC (1 and 10 mg/kg) when compared to kits treated with the free drug alone (Fig. 5B).

D-NAC therapy suppresses proinflammatory microglia

CD11b is expressed on the surface of activated microglia that are involved in inflammation and neurodegeneration. It is up-regulated by reactive oxygen species and plays a crucial role in exacerbating the neuroinflammatory process. CD11b expression is also associated with a change in morphology and motility of microglia (*36*). Brain sections from kits at day 5 were stained for all microglia with tomato lectin and for proinflammatory microglia with anti-CD11b antibody (Fig. 6A). CP kits treated with PBS had increased microglia staining compared to NAC- and D-NAC–treated groups, with most of the lectin-stained microglia colocalizing with CD11b, indicating the persistence of proinflammatory microglia in these animals on day 5 (Fig. 6, A and B). Treatment with D-NAC_10 resulted in a decrease in both total microglia and proinflammatory microglia (Fig. 6, A and B).

Staining for lectin further showed a change in microglial morphology, from an amoeboid (indicating activation of the microglia) to a more ramified form (normal microglial morphology), when treated with D-NAC_10 (Fig. 6A). Treatment with an equivalent dose of the drug (NAC_10) had no effect on CD11b expression, with microglial cells maintaining their amoeboid form similar to that seen with PBS treatment (Fig. 6, A and B). The persistence of activated, proinflammatory microglia along with increased expression of oxidative and inflammatory markers in the endotoxin kits treated with PBS (Fig. 5A) indicates that there is ongoing injury in the PVR in the postnatal period after a prenatal insult.

D-NAC therapy improves myelination and attenuates neuronal injury

Myelin basic protein (MBP) is one of the important structural proteins necessary for formation of myelin by mature oligodendrocytes. Neuroinflammation is associated with loss of myelination (*37*), resulting in the characteristic white matter injury seen in CP. A decrease in MBP staining is seen in the corona radiata, internal capsule, and external capsule by day 5 of life in endotoxin kits treated with PBS when compared to healthy controls (Fig. 7, A and B). A significant increase in myelin

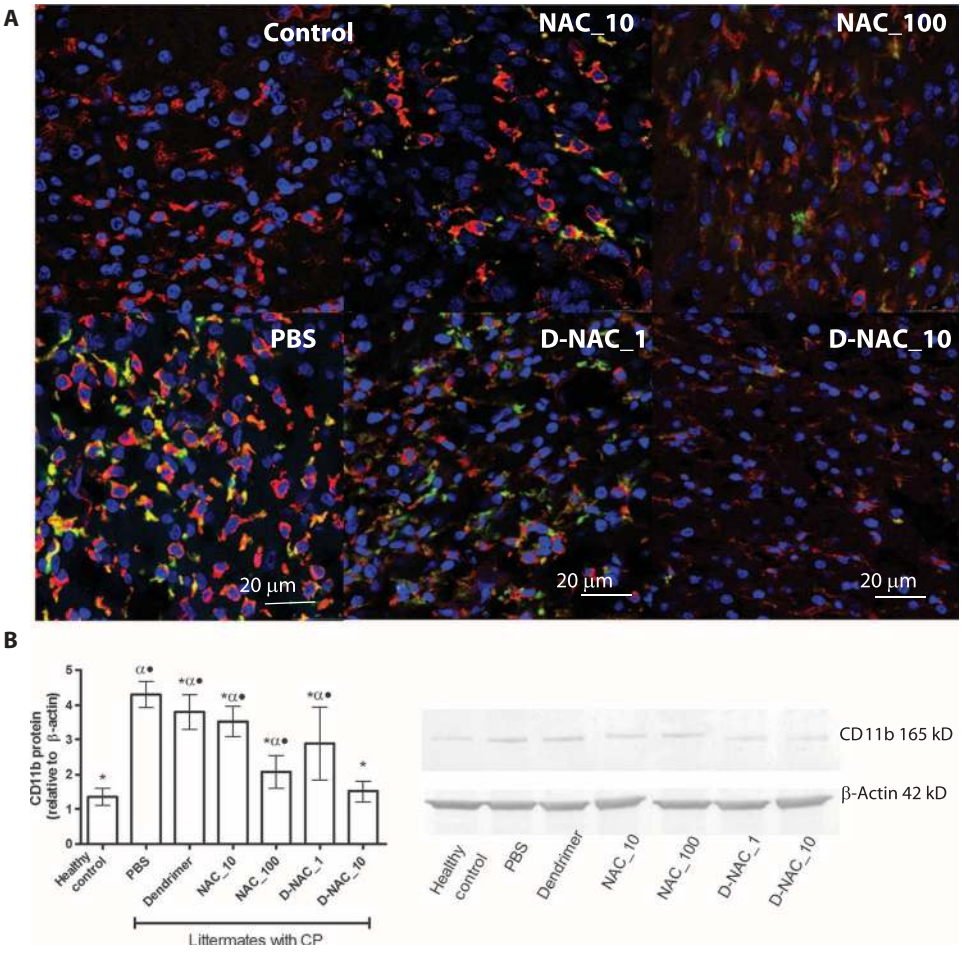

Fig. 6. Microglial response in the periventricular white matter region of rabbit kits on day 5 of life. (**A**) To detect a proinflammatory microglial phenotype, we stained brain sections using anti-CD11b (green). Tomato lectin (red) counterstain was used for microglial morphology. Merged areas appear yellow. Scale bars, 20 μm. (**B**) Western blot for CD11b and its quantification, with CD11b expression normalized to β-actin. Data are means with 95% CI for each group. $^*P < 0.05$ when compared to PBS; $^{\alpha}P < 0.01$ when compared to healthy control; $^{\bullet}P < 0.01$ when compared to D-NAC_10.

staining to almost healthy control levels is seen in the kits treated with D-NAC at 10 mg/kg (D-NAC_10), whereas the free drug at even 100 mg/kg (NAC_100) was less effective than D-NAC_10 (Fig. 7, A and B).

CP involves not only white matter injury but also neuronal apoptosis and neuron loss in areas such as the basal ganglia, which results in impaired coordination and motor control (*28*). Mature neurons were identified by staining for microtubule-associated protein 2 (MAP2) in the caudate region of the basal ganglia. Treatment with D-NAC (10 mg/kg) increased the number of neurons significantly compared to PBS, free NAC at 10 and 100 mg/kg, and D-NAC_1 ($P < 0.01$; Fig. 7C). A significant increase in neuronal counts was only seen in the D-NAC_10–treated CP group (Fig. 7C), with levels similar to healthy controls. The combination of improvement in myelination along with decreased neuronal cell loss may explain the marked improvement in motor function seen in animals treated with the dendrimer-drug conjugate when compared to treatment with a 10-fold higher dose of the free drug.

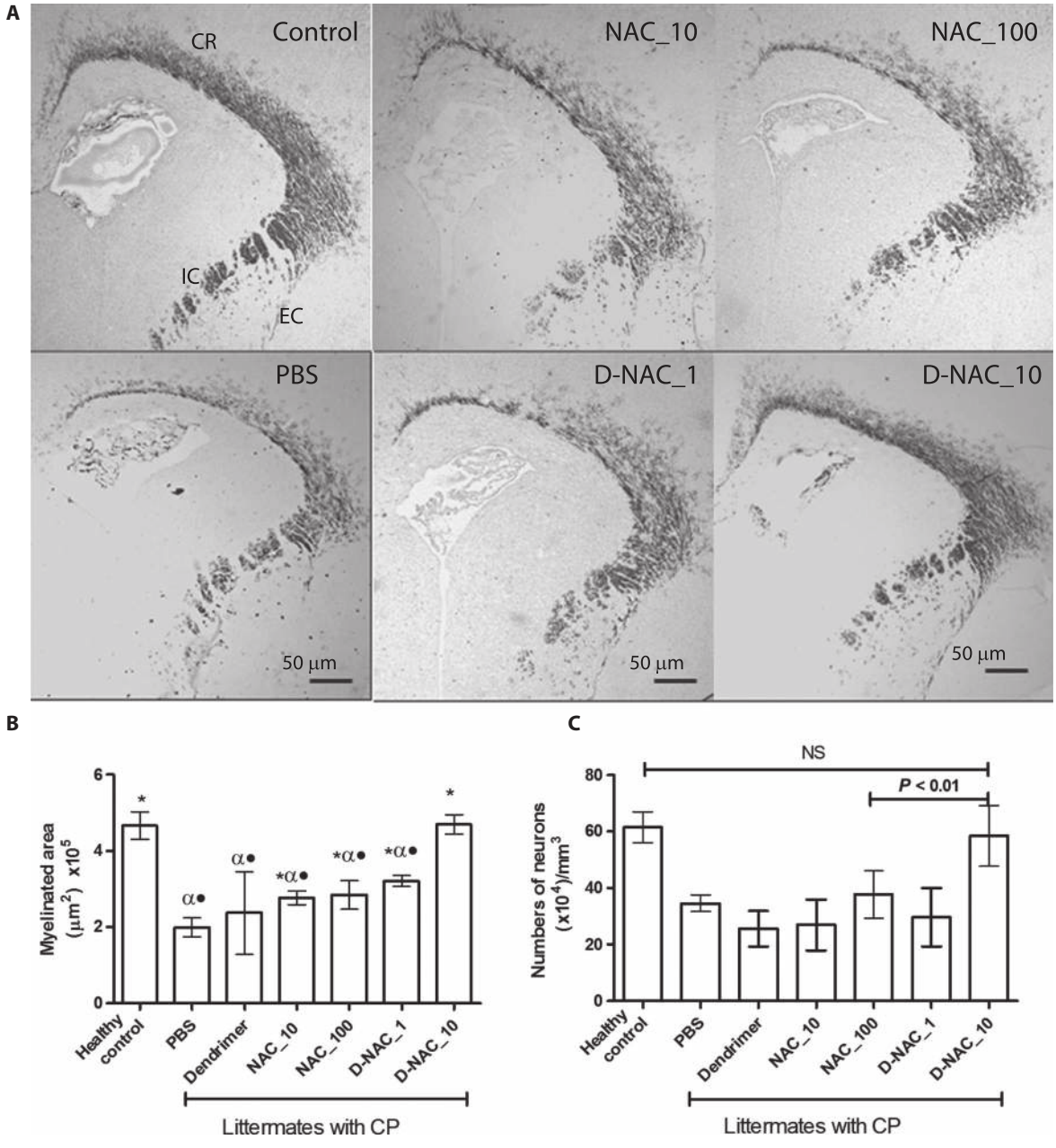

Fig. 7. Effect of therapy on myelination and neuronal injury. (**A**) Myelination in rabbit kits on day 5 of life. Representative brain sections stained for MBP. CR, corona radiata; EC, external capsule; IC, internal capsule. (**B**) Quantification of myelination. Data are means with 95% CI of the myelinated area per hemisphere. *$P < 0.05$ when compared to PBS; $^{\alpha}P < 0.01$ when compared to control; $^{\bullet}P < 0.01$ when compared to D-NAC_10. (**C**) Neuronal cell count in the caudate region of basal ganglia in the brains of newborn rabbits. Mature neurons were identified by MAP2 staining in the caudate region of the basal ganglia.

DISCUSSION

Current management for CP primarily focuses on rehabilitation and improving quality of life. Therapeutic approaches being explored include hypothermia for perinatal asphyxia and stem cell infusion for CP (*38*) (ClinicalTrials.gov IDs NCT01192776, NCT01147653, and NCT01072370). A key challenge in evaluating therapies for CP has been the paucity in animal models demonstrating the phenotype as seen in humans. The parallels in the timing of white matter development, along with microglial presence in the perinatal human and rabbit brain, make rabbit models of fetal brain injury more representative of CP in humans (*27*–*29*). The presence of activated microglia in the periventricular white matter, oxidative injury, impaired myelination, and neuronal loss seen in this model are consistent with histological findings seen in postmortem brain of patients with PVL (*8*). In addition, we find a predominance of hindlimb involvement in these animals, which is similar to the increased incidence of diparetic CP (involving lower extremities) in children born preterm to mothers with placental inflammation or infection (*6*).

We showed that systemic administration of hydroxyl-terminated PAMAM dendrimer resulted in their selective accumulation in activated microglia and astrocytes only in kits with CP. We attribute this increased brain and cell uptake in CP kits, to impairment of the BBB in the PVR, presumably leading to the increased permeability to dendrimers. This is consistent with previous reports of PAMAM dendrimers crossing the blood-brain-tumor barrier in models of malignant gliomas (*39*). An increase in the number of activated microglia and astrocytes, with enhanced phagocytic abilities under pathological conditions, may further facilitate the selective cellular localization of dendrimers in kits with CP (*40*). Technical and ethical considerations make direct evaluation of the BBB difficult in patients. However, studies in newborn animal models of white matter injury have shown increased permeability of the BBB in the presence of inflammation (*41*). Impairment of the BBB, in the presence of neuroinflammation, has also been reported in stroke, multiple sclerosis, and Alzheimer's disease (*42*). Passive targeting with dendrimers may facilitate delivery of therapeutics to neuroinflammation in these indications.

Intravenous administration of a single dose of D-NAC (10 mg/kg) resulted in a significant improvement in neuronal injury and motor function in CP kits (movie S3), whereas free NAC at 100 mg/kg did not, suggesting the importance of targeted drug delivery in the treatment of ongoing neuroinflammation. Although free NAC_100 showed some efficacy in attenuating inflammation and oxidative injury in the brain, the improvement did not translate to improved myelination, neuronal counts, or motor function. Moreover, the improvements seen with NAC_100 were similar to that seen with D-NAC at 1% of the dose (D-NAC_1). We speculate that this could be due to several factors, including poor bioavailability of free NAC (*43*), improved uptake and efficacy of D-NAC when compared to free NAC in activated microglia, as shown previously in vitro (*23*), delivery of a higher drug payload to the target cells (activated microglia and astrocytes) by the dendrimer in vivo, and decreased toxicity of the drug to neurons when conjugated with the dendrimer.

In the presence of inflammation and oxidative stress, depletion of GSH is one of the mechanisms by which the neuroprotective function of astrocytes is compromised (*12*). Regulated neuroglial transport of GSH and cysteine from astrocytes to neurons may play a role in neuroprotection (*44*). Hence, replenishing GSH specifically in astrocytes by D-NAC may help improve neuronal survival. In addition, excess extracellular L-cysteine concentrations have been shown to result in neuronal degeneration by NMDA (*N*-methyl-D-aspartate)–mediated excitotoxicity both in vitro and in vivo (*45*). Therefore, targeted delivery of the drug to activated microglia and astrocytes can not only help attenuate inflammation but may also prevent excess extracellular levels of L-cysteine produced from NAC that may be toxic to neurons and oligodendrocytes in the immature brain.

A therapeutic response was not seen upon treatment with dendrimer alone, which indicates that the dendrimer acts as a drug delivery vehicle. Although PAMAM dendrimers are not yet approved for clinical use, they are the subject of several preclinical studies (*16*, *19*). We use hydroxyl-terminated PAMAM dendrimers with a good safety profile in newborn kits, which may enable translation. In humans, because the exact time of the perinatal brain injury may vary, multiple injections of D-NAC or sustained release formulations may be needed for effective therapy. Future longitudinal studies focusing on long-term efficacy of this therapy up to adulthood will facilitate clinical translation. The platform described herein to target activated microglia and astrocytes has broad implications for the treatment of neurological diseases given the growing body of evidence that neuroinflammation plays a key role in the pathogenesis of disorders such as multiple sclerosis, Alzheimer's disease, and stroke. A similar therapeutic response with dendrimer-based targeting is also seen in models of retinal degeneration (*19*).

This work demonstrates that targeted attenuation of ongoing neuroinflammation can have significant implications for the treatment of maternal intrauterine infection and inflammation-induced brain injury, which leads to disorders such as CP. The effectiveness of the D-NAC treatment, administered in the postnatal period for a prenatal insult, suggests a new window of opportunity for the treatment of CP after birth in humans. Early detection of neuroinflammation using noninvasive, in vivo imaging techniques, such as PET and MRI (magnetic resonance imaging), can help in identifying patients at high risk for developing motor deficits in the newborn period (*26*, *30*). Targeted therapy for attenuation of neuroinflammation in at-risk patients, delivered at an early stage after birth, can potentially arrest or prevent the development of motor and cognitive deficits associated with perinatal brain injury and CP. Using dendrimers to deliver drugs to activated microglia and astrocytes may eventually provide a versatile platform for the treatment of other neuroinflammatory disorders.

MATERIALS AND METHODS

Rabbit model of CP

All animal procedures were approved by the Institutional Animal Care and Use Committee of Wayne State University and are as described previously (*26*, *27*, *30*). Timed pregnant New Zealand white rabbits were obtained from Covance Research Products Inc. Briefly, pregnant rabbits in the endotoxin group (n = 14 dams) underwent laparotomy at gestational day 28 (term pregnancy 31 days) and were injected with 1 ml of saline containing *Escherichia coli* endotoxin (20 μg/kg) (serotype O127: B8, Sigma Aldrich) along the length of the uterus (*26*, *27*). At this dose, the newborn kits have been shown to have uniform microglial activation in the PVR and display a phenotype of CP with predominantly hindlimb hypertonia (*26*, *27*, *30*). The healthy control group (n = 4 dams) included pregnant rabbits that had no surgery or intervention. All kits were born spontaneously on gestational day 31 and were used for the experiments.

Biodistribution of dendrimers in the brain

Newborn rabbit kits with CP (CP group, neuroinflammation, $n = 3$ from three different litters), and kits born to healthy rabbits that had no intervention (healthy control group, no neuroinflammation, $n = 3$ from three different litters), were intravenously administered D-FITC (10 mg/kg) on day 1 of birth and euthanized 24 hours later (*25*). For PET studies, newborn kits (controls, $n = 2$; CP kits, $n = 3$) were administered ^{64}Cu-dendrimer (or $^{64}CuCl_2$ control) intravenously on day 1 and imaged by PET after 24 hours.

Postnatal NAC therapy

A total of 69 kits from 14 dams in the endotoxin group were used for the different intravenous therapies. The kits were randomly distributed such that littermates (kits from the mother) were treated with either 200 μl of PBS (positive control; $n = 18$ kits from 11 mothers) or the same volume of PBS containing NAC_10 ($n = 10$ kits from six mothers), NAC_100 ($n = 11$ kits from eight mothers), D-NAC_1 ($n = 11$ kits from seven mothers), D-NAC_10 ($n = 12$ kits from six mothers), or dendrimer alone at a dose equivalent to that in D-NAC_10 ($n = 7$ kits from three mothers). To minimize potential variability among animals, we allocated kits from the same litter to different therapeutic interventions. The treatment groups were compared to control kits born to mothers that had no intervention (negative control, $n = 13$ kits from four mothers). These age-matched healthy controls (no intervention) were used for the comparison to demonstrate the extent of deviation from normal for the endotoxin kits and to compare response to treatment to see if it recovers to the level of the healthy control kits. This would simulate clinical studies where typical comparisons would be with completely healthy age-matched controls.

Behavioral testing

Newborn rabbits underwent neurobehavioral testing on days 1 and 5 of life with a modified scoring system, based on those described for rabbits (*28*). Because abnormalities in posture and movement are common manifestations in CP, the number of steps and hops taken was evaluated as an objective measure of motor function. Newborn kits were videotaped for 5 to 10 min and scored on the basis of the maximum number of steps and hops taken without falls during 1 min of continuous activity with the scoring system described below, by an operator masked to the treatment. The number of steps was scored from 0 to 4, with 0 for "drags or no steps, uses whole body to move, or not able to move"; 1 for "1 step or falls with almost every step"; 2 for "2 to 5 steps without falling"; 3 for "6 to 9 steps"; and 4 for "≥10 steps." The number of hops taken was scored similarly as 0 for no hops, 1 for "attempts to hop but falls," 2 for "one hop," 3 for "two to three hops," and 4 for "four or more hops." A "hop" was defined as lifting both hindlimbs off the ground to make a leap. Because normal, healthy rabbits do not hop on day 1 of life, the maximum possible score on day 1 was 4 and the maximum possible score on day 5 was 8. A detailed method for assessment of tone is provided in the Supplementary Methods.

Tissue isolation and preparation for analysis of oxidative injury and inflammation

For all tissue analysis, the region around the ventricles, where maximal neuroinflammation is seen in CP kits, was evaluated. The brain was sectioned in the coronal plane into 1-mm blocks. Then, the area around the ventricle, including parts of the corpus callosum, corona radiata, internal capsule, caudate, and dorsal hippocampus, was dissected from the level of the beginning of the lateral ventricle to the beginning of the dorsal hippocampus (denoted as the PVR), homogenized, and used for evaluation of oxidative injury, reverse transcription–polymerase chain reaction (RT-PCR), and Western blots. For all these measures, $n = 6$ to 7 kits from four litters (healthy controls), $n = 5$ to 11 kits from five to nine litters (endotoxin/PBS treatment), $n = 5$ kits from four litters (endotoxin/NAC_10), $n = 6$ kits from six litters (endotoxin/NAC_100), $n = 6$ kits from five litters (endotoxin/D-NAC_1), $n = 6$ kits from four litters (endotoxin/D-NAC_10), and $n = 4$ kits from three litters (endotoxin/dendrimer control).

GSH levels and oxidative injury

Commercially available immunoassays for GSH, 4-HNE, and NT-3 (Cell Biolabs Inc.) were validated and performed as per the manufacturer's instructions, after quantification of protein (Bradford) with the Coomassie protein assay kit. For the measurement of 8-OHG, a biomarker of oxidative injury to RNA, the OxiSelect Oxidative RNA Damage Kit (Cell Biolabs Inc.) was used. RNA samples extracted and purified with AllPrep DNA/RNA/Protein Mini Kit (Qiagen) were evaluated as per the manufacturer's instructions. All samples were run in duplicates.

Reverse transcription–PCR

Total RNA from brain tissue was purified (AllPrep DNA/RNA/Protein Mini Kit; Qiagen), quantified (NanoDrop ND-1000 Spectrophotometer; Thermo Scientific), and integrity-verified (Agilent 2100 Bioanalyzer with Eukaryote Total RNA Nanoassay). Single-stranded complementary DNA (cDNA) was reverse-transcribed from total RNA samples with the High-Capacity cDNA Reverse Transcription Kit with RNase inhibitor (Applied Biosystems), followed by PCR amplification with the TaqMan Universal Master Mix (Applied Biosystems). Primer sequences used were as follows: 5′-cttctgtctactgaacttcggggt-3′ (forward), 5′-tggaactgatgagagggagcc-3′ (reverse), and TGGAGTTCCGGATGTAT (probe) for TNF-α; 5′-cctacccccaatgtatccgttgtg-3′ (forward), 5′-ggaggaatgggagttgctgttgaa-3′ (reverse), and CACCCACTCCTCTACC (probe) for GAPDH (glyceraldehyde-3-phosphate dehydrogenase). Amplification conditions were the following: 30 min at 48°C, 10 min at 95°C, 40 cycles at 95°C for 15 s, and 60°C for 1 min. Samples were quantified with the ΔC_t (threshold cycle, amount of target = $2^{-\Delta\Delta Ct}$) method, normalized to the internal control gene *GAPDH*.

Western blot analysis

For analysis of NF-κB p65 and CD11b expression, nuclear and cytoplasmic extracts were prepared from brain tissue lysates with a nuclear extraction kit (Millipore) and separated on 4 to 12% NuPage Novex Bis-Tris MiniGels (Invitrogen). Proteins were transferred onto a polyvinylidene difluoride (PVDF) membrane and were probed with the following primary antibodies and dilutions: mouse anti-CD11b (1:100; AbD Serotec) and mouse anti–NF-κB p65 antibody (1:200; Abcam). Horseradish peroxidase (HRP)–conjugated goat anti-mouse secondary antibodies (1:500; Abcam) were used for detection. Expression of NF-κB and CD11b was developed with the electrochemiluminescence system (WesternBreeze Immunodetection Kit, Invitrogen) and x-ray photographic film (Eastman Kodak). The same blots were developed with WesternBreeze Chromogenic Kit (Invitrogen) for β-actin. The protein size was confirmed by molecular weight standards (Invitrogen). The integrated intensity for a fixed area of the bands for NF-κB, CD11b, and β-actin was obtained after background subtraction with ImageJ (National Institutes of Health). The values obtained for NF-κB and

CD11b were normalized to the β-actin from the same gel and expressed as ratios relative to the β-actin expression.

Immunohistochemistry

Staining protocols for colocalization of D-FITC with microglia and astrocytes have been previously described (*20*) (n = 10 to 12 sections per brain per kit; three kits per group).

Staining for CD11b, MBP, and MAP2

All protocols have been described previously (*26*, *27*, *30*, *46*). Sections were incubated with primary antibodies, mouse anti-rabbit CD11b (1:200; AbD Serotec), MBP (1:450; Covance), and MAP2 (1:500; Covance), followed by corresponding secondary antibodies, goat anti-mouse Alexa Fluor 488 (1:400; Invitrogen) or biotinylated goat anti-mouse (1:200; Vector Laboratories). For MAP2 and MBP, DAB staining was performed with ABC kit and developed by DAB peroxidase substrate kit (Vector Laboratories). For each of these markers, 4 to 7 brain sections per rabbit kit were stained and analyzed (n = 3 to 4 kits per group; 15 to 21 sections per group for each marker). Images were obtained with a Leica TCS SP-5 confocal microscope. Detailed methods for evaluation of BBB impairment with Evans blue dye and staining for occludin are provided in the Supplementary Methods.

Quantification of myelination and neuronal counts

For myelin quantification, 30-μm sections (five to seven sections, 120 μm apart; three to four kits per group) were evaluated at the level of bregma (1-mm anterior and 1-mm posterior). All images were captured with the same settings at ×10 magnification (Olympus) to cover the whole hemisphere. These images were processed and analyzed with Volocity software (Perkin Elmer), and myelinated areas were identified with the same threshold and object size limits for all images. Average area stained for myelin per hemisphere was obtained for each group. The number of neurons in the caudate nucleus was evaluated in every fifth section (four to five total sections per kit and three to four kits per group) from the beginning of the lateral ventricle to the end of dorsal hippocampus with an optical fractionator probe (Stereo Investigator). After the boundary of the caudate nucleus was defined by drawing a contour, MAP2-stained neurons were counted as previously described (*46*).

Statistical analysis

Because of the nesting of kits within litters and the repeated measurements for each kit, generalized estimating equations (GEE) was used to compare the outcomes between the groups (*47*). GEE accounts for the lack of independence that arises due to nesting of kits within a litter. GEE will also handle outcomes that are not normally distributed (for example, dichotomous data and count data) and data that are repeated across time. For assessment of neurobehavior on days 1 and 5, time was entered as a within-subjects variable as well as a predictor in the analyses. Modified Bonferroni corrections were applied to post hoc comparisons. All data are expressed as means and 95% CI obtained from the GEE analysis.

SUPPLEMENTARY MATERIALS

www.sciencetranslationalmedicine.org/cgi/content/full/4/130/130ra46/DC1

Materials and Methods

Fig. S1. Characterization of the D-NAC conjugate.

Fig. S2. Motor function evaluation of healthy rabbit kits at days 5 and 15.

Fig. S3. In vitro NAC release from D-NAC in PBS at various glutathione levels.

Fig. S4. PET images of ^{64}Cu-labeled dendrimer in control and CP kits 24 hours after tracer injection.

Table S1. Molecular weight, payload, and purity of D-NAC and its intermediates.

Table S2. Evaluation of liver and kidney function in healthy rabbit kits at days 5 and 15.

Table S3. Weight gain from day 1 to day 5 of life of treated newborn rabbits.

Movie S1. Healthy control kit on days 1 and 5 of life.

Movie S2. CP kit treated with PBS on day 1, videotaped on days 1 and 5.

Movie S3. CP kit treated with D-NAC_10 on day 1, videotaped on days 1 and 5.

Movie S4. CP kit treated with dendrimer (55 mg/kg) (vehicle control) on day 1, videotaped on days 1 and 5.

Movie S5. CP kit treated with NAC_10 on day 1, videotaped on days 1 and 5.

REFERENCES AND NOTES

1. P. Rosenbaum, N. Paneth, A. Leviton, M. Goldstein, M. Bax, D. Damiano, B. Dan, B. Jacobsson, A report: The definition and classification of cerebral palsy April 2006. *Dev. Med. Child Neurol. Suppl.* **109**, 8–14 (2007).
2. R. S. Kirby, M. S. Wingate, K. Van Naarden Braun, N. S. Doernberg, C. L. Arneson, R. E. Benedict, B. Mulvihill, M. S. Durkin, R. T. Fitzgerald, M. J. Maenner, J. A. Patz, M. Yeargin-Allsopp, Prevalence and functioning of children with cerebral palsy in four areas of the United States in 2006: A report from the Autism and Developmental Disabilities Monitoring Network. *Res. Dev. Disabil.* **32**, 462–469 (2011).
3. Centers for Disease Control and Prevention (CDC), Economic costs associated with mental retardation, cerebral palsy, hearing loss, and vision impairment—United States, 2003. *MMWR Morb. Mortal. Wkly. Rep.* **53**, 57–59 (2004).
4. A. Leviton, F. Gilles, Maternal urinary-tract infections and fetal leukoencephalopathy. *N. Engl. J. Med.* **301**, 661 (1979).
5. B. H. Yoon, R. Romero, J. S. Park, C. J. Kim, S. H. Kim, J. H. Choi, T. R. Han, Fetal exposure to an intra-amniotic inflammation and the development of cerebral palsy at the age of three years. *Am. J. Obstet. Gynecol.* **182**, 675–681 (2000).
6. A. Leviton, E. N. Allred, K. C. Kuban, J. L. Hecht, A. B. Onderdonk, T. M. O'Shea, N. Paneth, Microbiologic and histologic characteristics of the extremely preterm infant's placenta predict white matter damage and later cerebral palsy. The ELGAN study. *Pediatr. Res.* **67**, 95–101 (2010).
7. Y. W. Wu, G. J. Escobar, J. K. Grether, L. A. Croen, J. D. Greene, T. B. Newman, Chorioamnionitis and cerebral palsy in term and near-term infants. *JAMA* **290**, 2677–2684 (2003).
8. R. L. Haynes, R. D. Folkerth, R. J. Keefe, I. Sung, L. I. Swzeda, P. A. Rosenberg, J. J. Volpe, H. C. Kinney, Nitrosative and oxidative injury to premyelinating oligodendrocytes in periventricular leukomalacia. *J. Neuropathol. Exp. Neurol.* **62**, 441–450 (2003).
9. A. Monier, H. Adle-Biassette, A. L. Delezoide, P. Evrard, P. Gressens, C. Verney, Entry and distribution of microglial cells in human embryonic and fetal cerebral cortex. *J. Neuropathol. Exp. Neurol.* **66**, 372–382 (2007).
10. M. A. Dommergues, F. Plaisant, C. Verney, P. Gressens, Early microglial activation following neonatal excitotoxic brain damage in mice: A potential target for neuroprotection. *Neuroscience* **121**, 619–628 (2003).
11. J. Li, E. R. Ramenaden, J. Peng, H. Koito, J. J. Volpe, P. A. Rosenberg, Tumor necrosis factor α mediates lipopolysaccharide-induced microglial toxicity to developing oligodendrocytes when astrocytes are present. *J. Neurosci.* **28**, 5321–5330 (2008).
12. N. J. Maragakis, J. D. Rothstein, Mechanisms of disease: Astrocytes in neurodegenerative disease. *Nat. Clin. Pract. Neurol.* **2**, 679–689 (2006).
13. J. Brok, N. Buckley, C. Gluud, Interventions for paracetamol (acetaminophen) overdose. *Cochrane Database Syst. Rev.* **2**, CD003328 (2006).
14. X. Wang, P. Svedin, C. Nie, R. Lapatto, C. Zhu, M. Gustavsson, M. Sandberg, J. O. Karlsson, R. Romero, H. Hagberg, C. Mallard, *N*-Acetylcysteine reduces lipopolysaccharide-sensitized hypoxic-ischemic brain injury. *Ann. Neurol.* **61**, 263–271 (2007).
15. M. K. Paintlia, A. S. Paintlia, E. Barbosa, I. Singh, A. K. Singh, N-Acetylcysteine prevents endotoxin-induced degeneration of oligodendrocyte progenitors and hypomyelination in developing rat brain. *J. Neurosci. Res.* **78**, 347–361 (2004).
16. A. R. Menjoge, R. M. Kannan, D. A. Tomalia, Dendrimer-based drug and imaging conjugates: Design considerations for nanomedical applications. *Drug Discov. Today* **15**, 171–185 (2010).
17. M. Hayder, M. Poupot, M. Baron, D. Nigon, C. O. Turrin, A. M. Caminade, J. P. Majoral, R. A. Eisenberg, J. J. Fournié, A. Cantagrel, R. Poupot, J.-L. Davignon, A phosphorus-based dendrimer targets inflammation and osteoclastogenesis in experimental arthritis. *Sci. Transl. Med.* **3**, 81ra35 (2011).
18. C. C. Lee, J. A. MacKay, J. M. Fréchet, F. C. Szoka, Designing dendrimers for biological applications. *Nat. Biotechnol.* **23**, 1517–1526 (2005).
19. R. Iezzi, B. R. Guru, I. V. Glybina, M. K. Mishra, A. Kennedy, R. M. Kannan, Dendrimer-based targeted intravitreal therapy for sustained attenuation of neuroinflammation in retinal degeneration. *Biomaterials* **33**, 979–988 (2012).
20. H. Dai, R. S. Navath, B. Balakrishnan, B. R. Guru, M. K. Mishra, R. Romero, R. M. Kannan, S. Kannan, Intrinsic targeting of inflammatory cells in the brain by polyamidoamine dendrimers upon subarachnoid administration. *Nanomedicine* **5**, 1317–1329 (2010).

21. A. R. Menjoge, R. S. Navath, A. Asad, S. Kannan, C. J. Kim, R. Romero, R. M. Kannan, Transport and biodistribution of dendrimers across human fetal membranes: Implications for intravaginal administration of dendrimer-drug conjugates. *Biomaterials* **31**, 5007–5021 (2010).
22. R. S. Navath, Y. E. Kurtoglu, B. Wang, S. Kannan, R. Romero, R. M. Kannan, Dendrimer–drug conjugates for tailored intracellular drug release based on glutathione levels. *Bioconjug. Chem.* **19**, 2446–2455 (2008).
23. Y. E. Kurtoglu, R. S. Navath, B. Wang, S. Kannan, R. Romero, R. M. Kannan, Poly(amidoamine) dendrimer–drug conjugates with disulfide linkages for intracellular drug delivery. *Biomaterials* **30**, 2112–2121 (2009).
24. H. Kobayashi, M. W. Brechbiel, Nano-sized MRI contrast agents with dendrimer cores. *Adv. Drug Deliv. Rev.* **57**, 2271–2286 (2005).
25. S. Chatterjee, H. Noack, H. Possel, G. Keilhoff, G. Wolf, Glutathione levels in primary glial cultures: Monochlorobimane provides evidence of cell type-specific distribution. *Glia* **27**, 152–161 (1999).
26. S. Kannan, F. Saadani-Makki, O. Muzik, P. Chakraborty, T. J. Mangner, J. Janisse, R. Romero, D. C. Chugani, Microglial activation in perinatal rabbit brain induced by intrauterine inflammation: Detection with ^{11}C-(*R*)-PK11195 and small-animal PET. *J. Nucl. Med.* **48**, 946–954 (2007).
27. F. Saadani-Makki, S. Kannan, X. Lu, J. Janisse, E. Dawe, S. Edwin, R. Romero, D. Chugani, Intrauterine administration of endotoxin leads to motor deficits in a rabbit model: A link between prenatal infection and cerebral palsy. *Am. J. Obstet. Gynecol.* **199**, 651.e1–651.e7 (2008).
28. M. Derrick, N. L. Luo, J. C. Bregman, T. Jilling, X. Ji, K. Fisher, C. L. Gladson, D. J. Beardsley, G. Murdoch, S. A. Back, S. Tan, Preterm fetal hypoxia-ischemia causes hypertonia and motor deficits in the neonatal rabbit: A model for human cerebral palsy? *J. Neurosci.* **24**, 24–34 (2004).
29. G. Vinukonda, A. Csiszar, F. Hu, K. Dummula, N. K. Pandey, M. T. Zia, N. R. Ferreri, Z. Ungvari, E. F. LaGamma, P. Ballabh, Neuroprotection in a rabbit model of intraventricular haemorrhage by cyclooxygenase-2, prostanoid receptor-1 or tumour necrosis factor-alpha inhibition. *Brain* **133**, 2264–2280 (2010).
30. S. Kannan, F. Saadani-Makki, B. Balakrishnan, P. Chakraborty, J. Janisse, X. Lu, O. Muzik, R. Romero, D. C. Chugani, Magnitude of [^{11}C]PK11195 binding is related to severity of motor deficits in a rabbit model of cerebral palsy induced by intrauterine endotoxin exposure. *Dev. Neurosci.* **33**, 231–240 (2011).
31. K. Aoyama, M. Watabe, T. Nakaki, Regulation of neuronal glutathione synthesis. *J. Pharmacol. Sci.* **108**, 227–238 (2008).
32. H. Esterbauer, R. J. Schaur, H. Zollner, Chemistry and biochemistry of 4-hydroxynonenal, malonaldehyde and related aldehydes. *Free Radic. Biol. Med.* **11**, 81–128 (1991).
33. F. Groenendaal, H. Lammers, D. Smit, P. G. J. Nikkels, Nitrotyrosine in brain tissue of neonates after perinatal asphyxia. *Arch. Dis. Child. Fetal Neonatal Ed.* **91**, F429–F433 (2006).
34. X. Shan, Y. Chang, C. L. Lin, Messenger RNA oxidation is an early event preceding cell death and causes reduced protein expression. *FASEB J.* **21**, 2753–2764 (2007).
35. S. Oka, H. Kamata, K. Kamata, H. Yagisawa, H. Hirata, *N*-Acetylcysteine suppresses TNF-induced NF-κB activation through inhibition of IκB kinases. *FEBS Lett.* **472**, 196–202 (2000).
36. F. González-Scarano, G. Baltuch, Microglia as mediators of inflammatory and degenerative diseases. *Annu. Rev. Neurosci.* **22**, 219–240 (1999).
37. S. C. Zhang, B. D. Goetz, J. L. Carré, I. D. Duncan, Reactive microglia in dysmyelination and demyelination. *Glia* **34**, 101–109 (2001).
38. A. D. Edwards, D. V. Azzopardi, Therapeutic hypothermia following perinatal asphyxia. *Arch. Dis. Child. Fetal Neonatal Ed.* **91**, F127–F131 (2006).
39. H. Sarin, A. S. Kanevsky, H. Wu, K. R. Brimacombe, S. H. Fung, A. A. Sousa, S. Auh, C. M. Wilson, K. Sharma, M. A. Aronova, R. D. Leapman, G. L. Griffiths, M. D. Hall, Effective transvascular delivery of nanoparticles across the blood-brain tumor barrier into malignant glioma cells. *J. Transl. Med.* **6**, 80 (2008).
40. N. Choucair, V. Laporte, R. Levy, A. S. Arnold, J. P. Gies, P. Poindron, Y. Lombard, Phagocytic functions of microglial cells in the central nervous system and their importance in two neurodegenerative diseases: Multiple sclerosis and Alzheimer's disease. *CEJB* **1**, 463–493 (2006).
41. H. B. Stolp, K. M. Dziegielewska, C. J. Ek, M. D. Habgood, M. A. Lane, A. M. Potter, N. R. Saunders, Breakdown of the blood–brain barrier to proteins in white matter of the developing brain following systemic inflammation. *Cell Tissue Res.* **320**, 369–378 (2005).
42. H. E. de Vries, J. Kuiper, A. G. de Boer, T. J. Van Berkel, D. D. Breimer, The blood-brain barrier in neuroinflammatory diseases. *Pharmacol. Rev.* **49**, 143–155 (1997).
43. B. Olsson, M. Johansson, J. Gabrielsson, P. Bolme, Pharmacokinetics and bioavailability of reduced and oxidized N-acetylcysteine. *Eur. J. Clin. Pharmacol.* **34**, 77–82 (1988).
44. X. F. Wang, M. S. Cynader, Astrocytes provide cysteine to neurons by releasing glutathione. *J. Neurochem.* **74**, 1434–1442 (2000).
45. R. Janáky, V. Varga, A. Hermann, P. Saransaari, S. S. Oja, Mechanisms of L-cysteine neurotoxicity. *Neurochem. Res.* **25**, 1397–1405 (2000).
46. S. Kannan, F. Saadani-Makki, B. Balakrishnan, H. Dai, P. K. Chakraborty, J. Janisse, O. Muzik, R. Romero, D. C. Chugani, Decreased cortical serotonin in neonatal rabbits exposed to endotoxin in utero. *J. Cereb. Blood Flow Metab.* **31**, 738–749 (2011).
47. K. Y. Liang, S. L. Zeger, Longitudinal data analysis using generalized linear models. *Biometrika* **73**, 13–22 (1986).
48. R. S. Navath, A. R. Menjoge, B. Wang, R. Romero, S. Kannan, R. M. Kannan, Amino acid-functionalized dendrimers with heterobifunctional chemoselective peripheral groups for drug delivery applications. *Biomacromolecules* **11**, 1544–1563 (2010).
49. S. Kannan, B. Balakrishnan, O. Muzik, R. Romero, D. Chugani, Positron emission tomography imaging of neuroinflammation. *J. Child Neurol.* **24**, 1190–1199 (2009).
50. M. Kaya, S. Gulturk, I. Elmas, R. Kalayci, N. Arican, Z. C. Kocyildiz, M. Kucuk, H. Yorulmaz, A. Sivas, The effects of magnesium sulfate on blood-brain barrier disruption caused by intracarotid injection of hyperosmolar mannitol in rats. *Life Sci.* **76**, 201–212 (2004).
51. X. Chen, J. W. Gawryluk, J. F. Wagener, O. Ghribi, J. D. Geiger, Caffeine blocks disruption of blood brain barrier in a rabbit model of Alzheimer's disease. *J. Neuroinflammation* **5**, 12 (2008).
52. L. J. Gage, *Hand-Rearing Wild and Domestic Mammals* (Wiley-Blackwell, New York, 2002).

Acknowledgments: We thank M. Mishra (manuscript preparation), S. Kambhampati (drug release studies), and the PET Center at Wayne State University. **Funding:** Supported in part by the Perinatology Research Branch, Division of Intramural Research, *Eunice Kennedy Shriver* National Institute of Child Health and Human Development (NICHD), NIH, and by NICHD 5K08HD050652 (S.K.). **Author contributions:** S.K. was responsible for all animal studies, imaging, and efficacy assessment and provided the expertise in animal model development and cerebral palsy. H.D. was involved in animal surgeries and evaluation of inflammation and oxidative injury. R.S.N. prepared and characterized the dendrimer nanodevices. B.B. was involved in animal experiments and was responsible for neurobehavioral evaluation and neuronal injury assessment. A.J. was involved in evaluation of immunohistochemistry myelination. J.J. provided the statistical expertise. R.R. participated in the conception, research planning, data analysis, and manuscript writing. He also provided the expertise in perinatal medicine and cerebral palsy. R.M.K. was responsible for all aspects of dendrimer chemistry, characterization, formulation, and assessment of efficacy. S.K. and R.M.K. conceived the idea and were principal investigators responsible for directing and conducting the work, analysis and interpretation of data, and manuscript writing. All authors contributed to the writing of the manuscript. **Competing interests:** R.M.K., S.K., R.R., R.S.N., and H.D. have filed a patent (pending) (U.S. 12/797,657 and PCT/US10/38068).

Submitted 2 September 2011
Accepted 22 February 2012
Published 18 April 2012
10.1126/scitranslmed.3003162

Citation: S. Kannan, H. Dai, R. S. Navath, B. Balakrishnan, A. Jyoti, J. Janisse, R. Romero, R. M. Kannan, Dendrimer-based postnatal therapy for neuroinflammation and cerebral palsy in a rabbit model. *Sci. Transl. Med.* **4**, 130ra46 (2012).